

## LYMAN RESONANT SCATTERING IN YOUNG GALAXIES | PREDICTIONS FROM COSMOLOGICAL SIMULATIONS

Peter Laursen<sup>1</sup> and Jesper Sommer-Larsen<sup>1,2</sup>  
pela@dark-cosmology.dk, jschlarsen@tac.dk

Draft version July 2, 2019

## ABSTRACT

We present results obtained with a 3D, Ly $\alpha$  radiative transfer code, applied to a fully cosmological galaxy formation simulation. The developed Monte Carlo code is capable of treating an arbitrary distribution of source Ly $\alpha$  emission, neutral hydrogen density, temperature, and peculiar velocity of the interstellar medium. We investigate the influence of resonant scattering on the appearance and properties of young galaxies by applying the code to a simulated "Lyman Break Galaxy" at redshift  $z = 3.6$ , and of star formation rate  $22 \text{ M}_\odot \text{ yr}^{-1}$  and total Ly $\alpha$  luminosity  $2.0 \times 10^{43} \text{ erg s}^{-1}$ . It is found that resonant scattering of Ly $\alpha$  radiation can explain that young galaxies frequently are observed to be more extended on the sky in Ly $\alpha$  than in the optical. Moreover, it is shown that, for the system investigated, due to the anisotropic escape of the photons, the apparent maximum surface brightness can differ by a factor of 15, and the total derived luminosity by a factor of 4, depending on the orientation of the system relative to the observer.

Subject headings: galaxies: formation | radiative transfer | scattering | line: formation | line: profiles

## 1. introduction

The Ly $\alpha$  line is a very important diagnostic in a wide range of fields of astrophysics, not the least in galaxy formation, providing us with extensive information on redshift, dynamics, kinematics, morphology, etc. Three distinct physical processes result in Ly $\alpha$  "source" emission in the context of galaxies: Firstly, Ly $\alpha$  emission due to photo-ionization of hydrogen atoms by UV radiation from nearby, massive stars and subsequent recombinations may contribute as much as 10 % of the total luminosity of the galaxy (Partridge & Peebles 1967). Secondly, part of the potential energy gained by gas falling into galactic potential wells is converted into cooling radiation. Fardal et al. (2001) find that, at high redshifts, most of this radiation is emitted by gas with  $T < 20000 \text{ K}$ , and consequently

50% in Ly $\alpha$  alone. Finally, the external, intergalactic UV field, penetrating some (in case of Damped Lyman Alpha systems, DLAs) or all (in case of Lyman Limit Systems, LLSSs) of the outer parts of galactic hydrogen "envelopes" will also produce some Ly $\alpha$  radiation through case B recombination. In fact, approximately two-thirds of such recombinations will result in a Ly $\alpha$  photon (Spitzer 1978). Moreover, this UV field can also photo-heat non-self-shielded gas, which subsequently cools, radiating Ly $\alpha$  (Furlanetto et al. 2005).

Through the past years it has become possible to actually resolve observationally these young, Ly $\alpha$  emitting galaxies. In several cases, the galaxies have been found to be significantly more extended on the sky when observed in Ly $\alpha$  as opposed to optical bands (e.g., Moller & Warren 1998; Fynbo et al. 2001, 2003). Due to the complexity and diversity of the systems, in order to correctly interpret observations and make predictions about the properties of young galaxies, it is desirable to develop realistic theoretical/numerical models.

For a number of idealized cases analytical solutions are obtainable. Inspired by Unno (1955), Harrington (1973) investigated the emergent spectrum of resonantly scattered radiation in the case of a highly optically thick slab of finite thickness but infinite extension, and uniform temperature and density. He also gave a quantitative explanation of the fact discovered by Adams (1972) that the total number of scatterings that a photon undergoes before escaping the medium scales proportionally to the optical depth  $\tau_0$  in the line center and not, as one would naively expect from random walk considerations, as  $\tau_0^2$ . Neufeld (1990) extended this solution to include the possibility of the photons being destroyed (as by dust) and injected with arbitrary initial frequency. Dijkstra et al. (2005) derived a similar analytical expression for spherical symmetry, allowing for isotropic expansion or collapse of the gas, and Loeb & Rybicki (1999) examined the spectrum for an isotropically expanding or contracting medium with no thermal motion.

However, idealized these configurations may seem, they provide valuable and at least qualitative insight into the characteristics of young galaxies. Moreover, they offer direct means of testing numerical methods.

The Monte Carlo (MC) method was developed in the late 1940s (Metropolis & Ulam 1949), and has been used for solving radiative transfer (RT) problems since the beginning of the 1960s (Fleck 1963). Nevertheless, though conceptually simple, the demand for strong computer power until quite recently restricted this technique to deal with more or less the same idealized configurations that had already been dealt with analytically. Thus, the majority of previous attempts to model RT in astrophysical situations have been based on strongly simplified configurations.

## 2. simulations

<sup>1</sup> Dark Cosmology Centre, Niels Bohr Institute, University of Copenhagen, Julianehåb Vej 30, DK-2100, Copenhagen, Denmark.<sup>2</sup> Institute of Astronomy, University of Tokyo, Osawa 2-21-1, Mitaka, Tokyo, 181-0015, Japan.

## 2.1. The Cosmological Simulation and Monte Carlo Code

The cosmological simulation of the formation and evolution of an individual galaxy was performed using the N-body/hydrodynamical TreeSPH code, briefly described in Sommar-Larsen (2006, for a more thorough description, see Sommar-Larsen et al. (2003)). The system becomes a Milky Way/M 31-like disk galaxy at  $z = 0$  and is simulated using about 2.2 million particles in total, comprising only smoothed particle hydrodynamical (SPH) and dark matter (DM) particles at the initial redshift  $z_i = 39$ . The masses and gravity softening lengths of SPH and star particles are  $9.9 \cdot 10^4 h^{-1} M_\odot$  and  $200 h^{-1} \text{ pc}$ , respectively ( $h = 0.65$ ). For the DM particles the corresponding values are  $5.7 \cdot 10^5 h^{-1} M_\odot$  and  $370 h^{-1} \text{ pc}$ . The minimum SPH smoothing length in the simulation is about  $13 h^{-1} \text{ pc}$ . For the purposes of the present study, a single simulation output, at  $z = 3.6$ , was chosen.

The MC code, used to propagate the photons through the medium, by and large resembles those recently developed by other authors (e.g., Cantalupo et al. 2005; Tasitsiomi 2006). Since it is grid-based (the number of cells typically being  $512^3$ ) the physical parameters of interest are first interpolated from the gas particles of the SPH simulation to the cells of the computational box. These parameters are the Lyman emissivity  $l_{\text{Ly}}$ , the temperature  $T$ , the density  $n_{\text{H}_1}$  of neutral hydrogen, and the three dimensional velocity field  $v_{\text{bulk}}$  of the gas.

## 2.2. Determination of "Source" Lyman Emission

The emission cell of a given Lyman photon is found by setting the probability of being emitted from a given cell equal to the ratio of the luminosity in that cell to the total luminosity  $L_{\text{tot}}$ . The photon is then injected in the line center (in the reference frame of the medium) from a random point  $x_i$  in the cell. Following most earlier work on the subject, the frequency of the photon is parametrized through  $x = (v_0) = \frac{v_{\text{th}}}{v_{\text{D}}}$ , where  $v_0 = 2.466 \cdot 10^{15} \text{ Hz}$  is the line center frequency and  $v_{\text{D}} = (v_{\text{th}} = c) v_0$  is the Doppler frequency, with  $v_{\text{th}} = (2k_B T / m_{\text{H}})^{1/2}$  being the thermal atom velocity dispersion (in  $\text{m s}^{-2}$ ) and the rest of the variables having their usual meanings. In terms of this variable the injected photon obviously has a frequency of  $x = 0$ . The initial direction  $\hat{n}_i$  of the photon follows an isotropic probability distribution.

## 2.3. Propagation of the Radiation

The optical depth covered by the photon before it is scattered is drawn randomly from the probability distribution  $e^{-x}$ , and subsequently converted into a physical distance  $r = -n_{\text{H}_1} x$ . The cross-section  $x$  is given by a Voigt profile, i.e. the convolution of the Lorentzian natural line profile and the Gaussian thermal broadening of the atoms, resulting in

$$x = f_{12} \frac{p - e^2}{m_e c} H(a; x); \quad (1)$$

where  $f_{12} = 0.4162$  is the Lyman oscillator strength, and

$$H(a; x) = \frac{a}{1} \int_{Z+1}^{\infty} \frac{e^{-y^2}}{(x - y)^2 + a^2} dy \quad (2)$$

is the Voigt function with  $a = \frac{v_{\text{th}}}{v_{\text{D}}} = 2$ , the ratio between the natural line width  $\frac{v_{\text{th}}}{v_{\text{D}}} = 9.936 \cdot 10^7 \text{ Hz}$  and the Doppler width. Since eq. (2) is not analytically integrable, we use the analytic fit given by Tasitsiomi (2006) which is a very good approximation for all frequencies at temperatures above 2 K.

If the final position  $x_f$  of the photon is outside the original cell, the photon is placed at the point  $x_{\text{int}}$  of intersection with the face of the cell and the above calculation is redone with the parameters of the new cell, an optical depth

$\tau = \int_{x_{\text{int}}}^{x_f} x_{ij} (n_{\text{H}_1} x)_{\text{prev cell}}$ , and a frequency Lorentz transformed to the bulk velocity of the new cell. This procedure is repeated until either the originally assigned value of  $\tau$  is spent, and the photon is scattered, or it leaves the computational box.

## 2.4. Scattering

Except for a small recoil effect, the scattering is coherent in the reference frame of the atom. However, to an external observer, the non-zero velocity  $u = v_{\text{atom}} - v_{\text{th}}$  of the atom will shift the frequency of the photon. In the directions perpendicular to  $\hat{n}_i$ , the velocities  $u_{\perp,1}$  and  $u_{\perp,2}$  will follow a Gaussian distribution. When  $x = 0$ , the photon barely disperses spatially. Only when it has dispersed sufficiently far in frequency space, it will be able to make a large journey in real space. To skip these non-important core scatterings and thus accelerate the code, if  $|x|$  is less than some critical value  $x_{\text{crit}}$ , following Dijkstra et al. (2005)  $u_{\perp,1,2}$  is drawn from a truncated Gaussian so as to favor fast moving atoms and artificially push the photon back in the wing.  $x_{\text{crit}}$  is determined according to a  $\alpha$  in the given cell. If  $\alpha < 1$ , a proper Gaussian is used; otherwise we find that  $x_{\text{crit}} = 0.02 e^{-\ln \alpha}$ , where  $(\alpha) = (0.6; 1.2)$  or  $(1.4; 0.6)$  for  $\alpha > 60$  or  $\alpha < 60$ , respectively, can be used without affecting the final result. The effect of this acceleration scheme is a speed-up of several orders of magnitude. Due to the resonance nature of the scattering event, for small values of  $|x|$  being scattered by an atom with  $u_{\perp,j} = x$  is highly favored. For large values of  $|x|$  the abundance of these atoms decrease as  $e^{-x^2}$ , so that scattering by "slow" atoms becomes more probable, even though in reference frame of these atoms the photon is far in the wing. The resulting normalized probability distribution is

$$f(u_{\perp,j}) = \frac{a}{H(a; x)} \frac{e^{-u_{\perp,j}^2}}{(x - u_{\perp,j})^2 + a^2}; \quad (3)$$

We generate  $u_{\perp,j}$  from this distribution following Zheng & Miralda-Escude (2002). As the value  $u_0$  separating the two comparison functions (Zheng & Miralda-Escude 2002), for the wide range of temperatures and frequencies involved, we find that a satisfactory average acceptance-to-rejection ratio of approximately 1=4 is achieved for

$$u_0 = \begin{cases} 0 & \text{for } 0 < x < 0.2 \\ x - ae^{1.2x+b} - 0.5 \sin(2x) = 5 & \text{for } 0.2 < x < Q(a) \\ 4.5 & \text{for } x > Q(a); \end{cases} \quad (4)$$

where  $b = 0.84 \ln a - 4.4$ , and

$$Q(a) = 0.0283 \ln^2 a - 0.514 \ln a + 3.648; \quad (5)$$

The final frequency  $x^0$  of the scattered photon (in the observers frame) depends on direction in which the photon

is scattered. For scattering in the line center, transitions to the  $2P_{1=2}$  state results in isotropic scattering, while the  $2P_{3=2}$  transition causes some polarization, resulting in a probability distribution  $W(\theta) / 1 + \frac{3}{7} \cos^2 \theta$ , where  $\theta$  is the angle between  $\hat{n}_i$  and the outgoing direction  $\hat{n}_f$  (Hamilton 1940). Since the spin multiplicity is  $2J + 1$ , the probability of being excited to the  $2P_{3=2}$  state is twice as large as being excited to the  $2P_{1=2}$  state<sup>3</sup>. For scatterings in the wing, polarization for  $J=2$  scattering is maximal, resulting in a dipole distribution  $W(\theta) / 1 + \cos^2 \theta$  (Stenflo 1980). The transition from core to wing scattering is given by the value of  $x$  where the Lorentzian starts dominating the Gaussian profile, i.e. where  $a = x^2 - e^{-x^2}$ , or  $x = 3$  (the exact value is not crucial). In all cases, the scattering is isotropic in the azimuthal angle. In the observers frame, the final frequency is then given by

$$x^0 = x \cdot u_{jj} + \hat{n}_f \cdot u + g(1 - \hat{n}_f \cdot \hat{n}_i); \quad (6)$$

where the factor  $g = h_{p10} = m_H c v_{th}$  (Field 1959) accounts for the recoil effect.

## 2.5. Transforming to Observable Surface Brightness Maps

Following the above scheme, the photons are propagated through the medium, one by one, until they escape the computational box. For each scattering (as well as the emission) of a photon we calculate the probability that the photon will escape in the direction of six virtual observers situated in the negative and positive directions of the three principal axes. This probability is added as a weight to a three dimensional array (the two spatial dimensions of the projected image of the galaxy, plus a spectral dimension for each pixel). The array is finally collapsed along the spectral dimension and along the spatial dimensions to yield the image and spectrum, respectively, that an external observer would see. The contribution of each pixel element to the surface brightness<sup>4</sup> (SB) is then

$$SB_{pix} = \frac{L_{tot}}{n_{ph}} \frac{1}{d_L^2} \frac{1}{\Omega_{pix}} e^{-\tau_{ph;scat}} \quad (7)$$

where  $n_{ph}$  is the number of photons,  $d_L$  is the luminosity distance to the observer,  $\Omega_{pix}$  is the solid angle subtended by the pixel, and  $\tau_{scat}$  is the optical depth of the gas lying between the scattering event and the edge of the computational box in the direction of the observer.

The MC code was tested on various simple configurations for which analytic solutions exist, discussed in the introduction. Our code exquisitely passes all tests. We will present the results of these tests in a future paper.

## 3. results

We apply the MC code to a proto-galaxy at  $z = 3.6$ , consisting of two small, star forming "disks" separated by approximately 2 kpc, on one of which the computational box is centered, and a third more extended, but lower star formation rate (SFR) disk, located about 15 kpc from the center. In addition, the star forming regions are embedded in a significant amount of more diffuse, non-star

<sup>3</sup> For the environments produced here, transitions to the  $2S$  state and subsequent destruction of the photon can be neglected.

<sup>4</sup> measured in  $\text{erg s}^{-1} \text{cm}^{-2} \text{arcsec}^{-2}$  at the location of the observer.

<sup>5</sup> These numbers are determined from a non-accelerated (i.e.  $x_{crit} = 0$ ) run of the code with a few  $10^3$  photons.

forming, H I gas in a 10–15 kpc thick, sheet-like structure, taken to constitute the  $xy$ -plane. The total SFR of the system is  $22 \text{ M}_\odot \text{ yr}^{-1}$ . Observed Lyman B break Galaxies (LBGs) have SFRs in the range  $10$ – $1000 \text{ M}_\odot \text{ yr}^{-1}$  (e.g., Rigopoulou et al. 2006), so the simulated galaxy corresponds to a small LBG. The length of the box used for the MC calculations is 50 kpc (physical), and  $d_L = 34 \text{ Gpc}$ . Fig. 1 shows the results obtained, viewed from two different directions: from the negative  $x$ - and  $z$ -direction, corresponding to an edge-on and a face-on view of the sheet-like structure, respectively. Upper panels assume that the gas is optically thin to the Lyman line, lower show the corresponding results with resonant scattering included. The effect of the scattering is incontestable: Although the original constellation of the principal emitters is still visible, the surface brightness distribution is clearly much more extended. Moreover, we notice the effect of the viewing angle. Qualitatively, we expect the photons to escape more easily from the face of the sheet than from the edge and hence that the system should have a higher surface brightness when viewed edge-on. We quantify this anticipation: Fig. 2 shows the azimuthally averaged SB profiles. To allow for direct comparison with observations, the profiles are also shown not including the luminosity of the emitter lying in the outskirts of the image and smoothed with a PSF corresponding to a seeing of  $0.8''$ . The maximum SB of the  $xy$ -plane is found to be  $6.6 \cdot 10^{-2} \text{ erg s}^{-1} \text{ cm}^{-2}$ , or

17 times higher than that of the  $yz$ -plane. The average SB, from which the total luminosity is usually derived assuming isotropic emission, is 3.8 times higher.

Finally, we show the emergent spectrum. Though not as clear for the edge-on view, both profiles exhibit the characteristic double-hump peak profile (see, e.g., Venemans et al. 2005). Obviously, this is the result of the high opacity for photons near the line center; diffusing to either side of  $\theta = 0$  quickly decreases so as to make escape more probable. Furthermore, both profiles imply a net inward velocity of the gas; for infalling gas, red photons are shifted into resonance, while blue photons escape even more easily, thus enhancing the blue peak and diminishing the red.

Fitting a "Nuerfeld profile" to the observed spectra can give us an idea of the intrinsic characteristics of the system. Unfortunately, there is a degeneracy in that the profile is dependent only on the parameter  $a_0$ . Assuming some temperature, e.g.  $10^4 \text{ K}$ , representative of most of the Lyman emitting gas, one could in principle deduce the equivalent column density  $N_{\text{H}_2}$ . Alternatively, if  $N_{\text{H}_2}$  is obtainable due to, e.g., the presence of a background quasar, constraints can be put on the temperature.

A bulk rotational motion of the gas will also alter the profile. Since in fact a full spectrum is obtained for every pixel element, this effect can be studied through long slit spectroscopy.

## 4. discussion and conclusion

The present MC calculations do not include the effect of dust. Effectively, dust will act as a photon sink and an extra scattering possibility. Since, on average, each photon scatters  $4 \cdot 10^8$  times and travel a distance of  $\sim 40$

kpc before escaping<sup>5</sup>, approximately half of which is in the high density ( $n_{H_1} \approx 0.1 \text{ cm}^{-3}$ ), cooler ( $T \approx 10^4 \text{ K}$ ) regions, we expect even a small amount of dust to be able to cause a significant decrease in the observed intensity. However, it is not clear to which extend the dust will affect the observations. If the medium is clumpy, the ratio of Ly to continuum radiation may in fact be increased (Neufeld 1991; Hansen & Oh 2006). Moreover, Tasitsiomi (2006) argues that dust acting as catalyst for hydrogen molecules will lower  $n_{H_1}$ , making the medium more transparent. We will study these effects in future work, implementing a realistic model of the dust based on the 8 different metal species kept track of by the cosmological simulation.

As a very recent improvement of the cosmological simulation, a post-processed RT scheme of UV radiation from star forming regions was developed by Razoumov & Sommer-Larsen (2006). They find that up to 5–10% of the ionizing photons escape these regions at  $z = 3.6$ . However, a very preliminary analysis indicates

that the results presented in this work are not significantly changed by the inclusion of H ionizing photon RT. The quantitative effects of this on Ly RT will also be discussed in a forthcoming paper.

The developed Monte Carlo code has reproduced qualitatively and quantitatively the observation that young galaxies often appear significantly more extended on the sky in Ly than in the optical. Furthermore, we have investigated the impact of the viewing angle on the observed surface brightness. Future simulations of a large statistical sample of galaxies, taking properly into account dust and H ionizing UV photon radiative transfer, will allow us to learn more about the enigmatic Ly emitters.

The authors are very grateful to J. Fynbo and T. Haugbølle for beneficial discussions, to A. Tasitsiomi for quick response to questions, and to J. Schaye for useful comments. The simulations were performed on the SGII Itanium II facility provided by DCSC. The Dark Cosmology Centre is funded by the DNRF.

#### REFERENCES

Adams, T. F. 1972, *ApJ*, 174, 439  
 Cantalupo, S., Porciani, C., Lilly, S. J., & Minati, F. 2005, *ApJ*, 628, 61  
 Dijkstra, M., Haiman, Z., & Spaans, M. 2005, *astro-ph/0510407*  
 Fardal, M. A., Katz, N., Gardner, J. P., Hemquist, L., Weinberg, D. H., & Davé, R. 2001, *ApJ*, 562, 605  
 Field, G. 1959, *ApJ*, 129, 551  
 Fleck, J. A., Jr. 1963, *Methods in Computational Physics*, Vol. I, ed. B. Alder, S. Farnbach, & M. Rotenberg (New York: Academic Press)  
 Furlanetto, S. R., Schaye, J., Springel, V., Hemquist, L. 2005, *ApJ*, 622, 7  
 Fynbo, J. P. U., Møller, P., & Thomsen, B. 2001, *A&A*, 374, 443  
 Fynbo, J. P. U., Ledoux, C., Møller, P., Thomsen, B. & Burud, I. 2003, *A&A*, 407, 147  
 Hamilton, D. R. 1940, *Phys. Rev.*, 58, 122  
 Hansen, M., & Oh, S. P. 2006, *MNRAS*, 367, 979  
 Harrington, J. P. 1973, *MNRAS*, 162, 43  
 Loeb, R., & Rybicki, G. B. 1999, *ApJ*, 524, 527  
 Metropolis, N., & Ulam, S. 1949, *Journal of the American Statistical Association*, 44 (247), 335  
 Møller, P., & Warren, S. J. 1998, *MNRAS*, 299, 611  
 Neufeld, D. 1990, *ApJ*, 350, 216  
 Neufeld, D. 1991, *ApJ*, 370, L85  
 Partridge, R. B., & Peebles, P. J. E. 1967, *ApJ*, 147, 868  
 Razoumov, A. O., & Sommer-Larsen, J. 2006, *ApJ*, accepted (astro-ph/0609545)  
 Rigopoulou, D., et al. 2006, *ApJ*, 648, 81  
 Sommer-Larsen, J., Gottz, M., & Portinari, L. 2003, *ApJ*, 596, 47  
 Sommer-Larsen, J. 2006, *ApJ*, 644, L1  
 Spitzer, L. 1978, *Physical Processes in the Interstellar Medium* (New York: Wiley-Interscience)  
 Stenflo, J. O. 1980, *A&A*, 84, 68  
 Tasitsiomi, A. 2006, *ApJ*, 645, 792  
 Unno, W. 1955, *PASJ*, 7, 81  
 Venemans, B., et al. 2005, *A&A*, 431, 793  
 Zheng, Z., & Miralda-Escude, J. 2002, *ApJ*, 578, 33

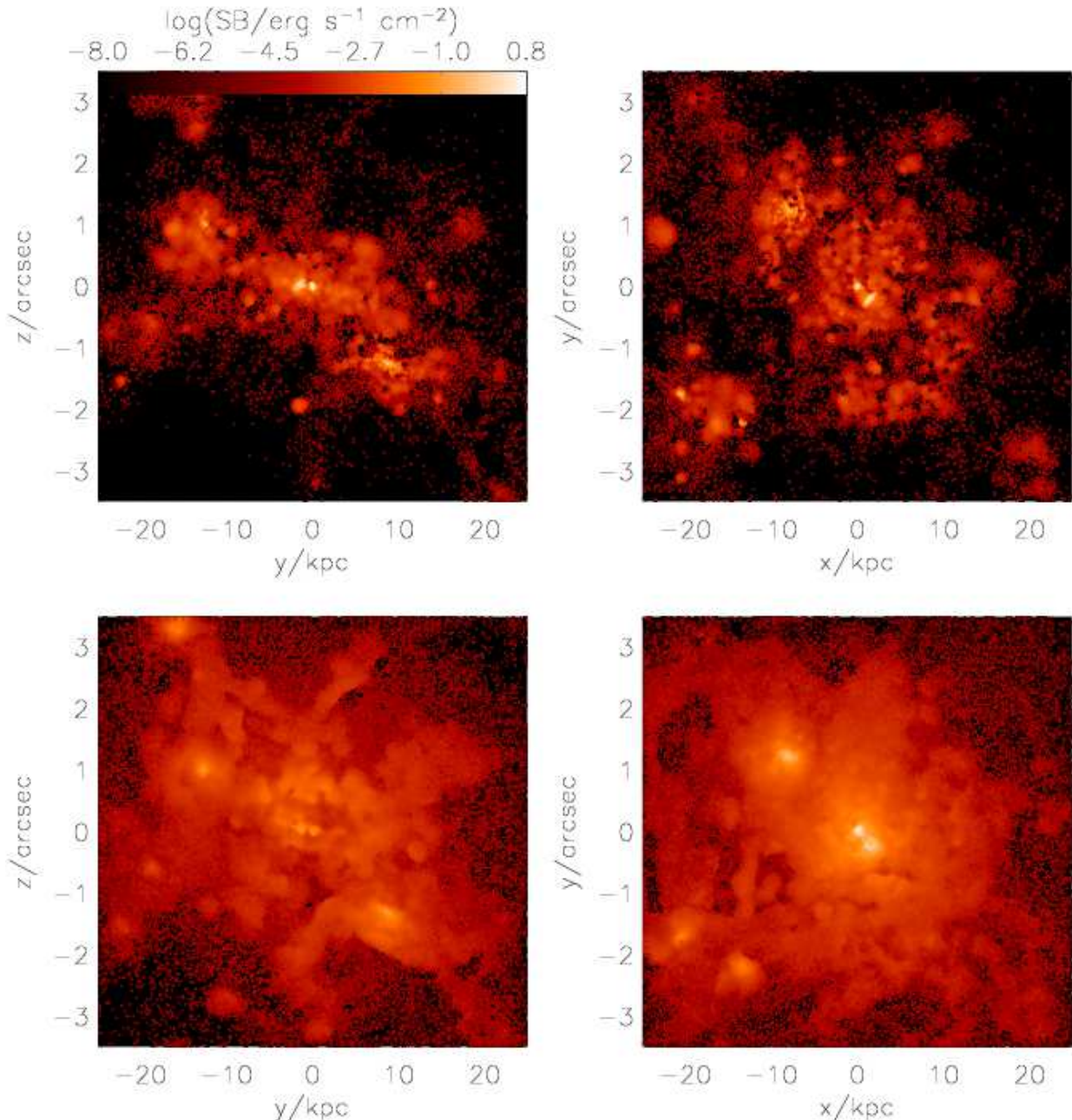


Fig. 1.1| Bolometric surface brightness map of a simulated galaxy at  $z = 3.6$ . Left and right column show the system when viewed edge-on and face-on, respectively. The top panel displays the galaxy as if the Lyman-alpha radiation was able to escape directly, without scattering. The bottom panel shows the effect of the scattering.

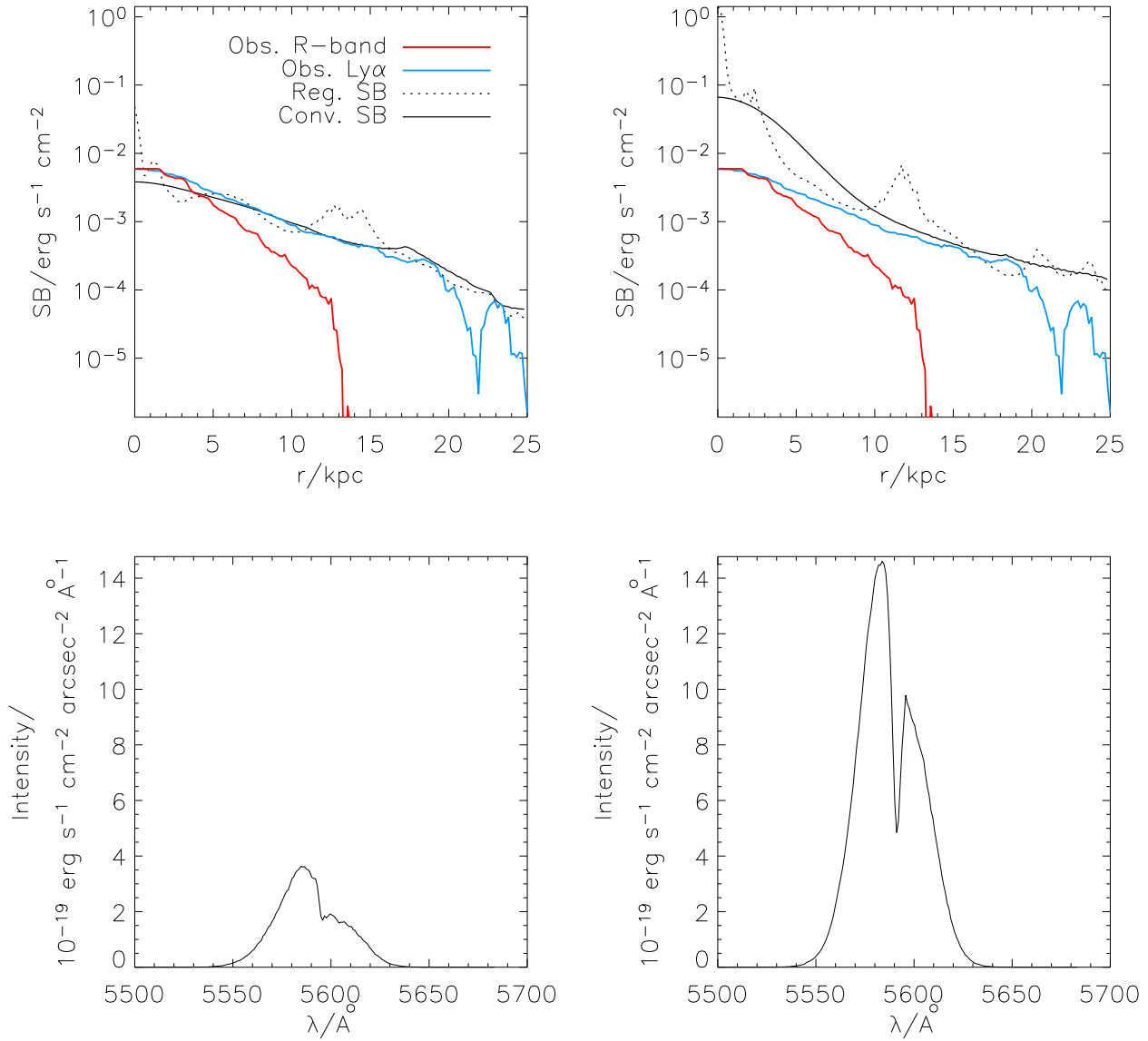


Fig. 2.1. Surface brightness (SB) profiles and emergent spectrum of the galaxy. Left and right column show the system when viewed edge-on and face-on, respectively. In the top panel, the true SB profiles (dotted lines) and the profiles convolved with a seeing of  $0.8''$  and convolving the luminosity of the remote emitters (solid lines) are displayed. Also shown are the SB profiles of the galaxy LEG O 2138-29 (SFR  $15 \text{ M}_\odot \text{ yr}^{-1}$  if extinction is negligible, Fynbo et al. 2003) in Ly $\alpha$  (blue) and in the R-band (red, normalized to the maximum observed Ly $\alpha$  SB). In particular the SB of the  $yz$ -plane nicely reproduces the observed SB. Left axes measure the SB at the source, while right axes measure the SB observed at  $z = 0$ . The bottom panel shows the emergent spectrum, clearly displaying the characteristic double-hump profile. The enhanced blue peak indicates a net inward bulk velocity of the gas.